

# Isobaric Vapor–Liquid and Liquid–Liquid Equilibria for Chloroform + Ethanol + 1-Ethyl-3-methylimidazolium Trifluoromethanesulfonate at 100 kPa

A. Vicent Orchillés, Pablo J. Miguel, Ernesto Vercher, and Antoni Martínez-Andreu\*

Departamento de Ingeniería Química, Escuela Técnica Superior de Ingeniería, Universitat de València, 46100 Burjassot, Valencia, Spain

Isobaric vapor–liquid equilibria for the binary systems chloroform + ethanol and chloroform + 1-ethyl-3-methylimidazolium trifluoromethanesulfonate ([emim][triflate]) as well as the vapor–liquid equilibria for the chloroform + ethanol + [emim][triflate] ternary system have been obtained at 100 kPa using a recirculating still. Both binary and ternary systems containing ionic liquid present an immiscibility zone at high chloroform composition, which increases with temperature. Also, liquid–liquid equilibria for both systems have been determined. The measured ternary VLE data were correlated using Mock's electrolyte NRTL model which reproduces reasonably well the experimental values. The detected immiscibility does not affect the use of [emim][triflate] as an entrainer for the complete chloroform + ethanol separation, and the azeotrope has totally disappeared when the mole fraction of ionic liquid in the liquid phase is 0.21.

## Introduction

Distillation is a widely used industrial process for separation that becomes highly restricted when azeotropes appear. Nevertheless, azeotropes can be broken by addition of an entrainer (solvent or salt) which modifies the relative volatility and makes the separation more efficient. However, the use of salts presents problems associated with their causticity and limited solubility in organic compounds, whereas solvents may contaminate the product streams.

Ionic liquids (ILs) are substances formed by relatively large organic cations and inorganic or organic anions which have melting points around ambient temperature and behave as electrolytes besides showing a relative low viscosity and good stability up to 200 °C being, at the same time, much less corrosive than conventional fused salts.<sup>1</sup>

In this way, ILs are said to have significant processing advantages as entrainers when used in extractive distillation.<sup>2</sup> Indeed, they have practically no vapor pressure which makes it easier for us to obtain noncontaminated distillate and bottom fractions. They are liquid at work temperature which avoids the problems associated with the handling of fused or solid salts, and what is more, since solubility of ILs in polar and nonpolar substances can be customized,<sup>3</sup> the mole concentration of the electrolyte inside the distillation column can be increased giving a stronger salt effect.

Arlt and co-workers<sup>4–8</sup> first suggested using ILs for separation in azeotropic mixtures. However and in spite of the apparent success of such innovation, currently there are not too many investigations about the effect of ILs on vapor–liquid equilibria. Moreover, in most cases, the studies on the vapor–liquid equilibria of IL-containing systems are uncompleted because they are limited to determining the vapor pressure and/or activity coefficients of one or two solvents in ILs. Only Zhao et al.<sup>9,10</sup> (ethanol + water, ethanol + methanol), Calvar et al.<sup>11–13</sup> (ethanol + water), Orchillés et al.<sup>14–17</sup> (acetone + methanol,

methyl acetate + methanol, ethyl acetate + ethanol, 1-propanol + water), Zhang et al.<sup>18–20</sup> (water + 2-propanol, water + 1-propanol, water + ethanol + ethyl acetate), and Li et al.<sup>21</sup> (2-propanol + water) have reported complete isobaric vapor–liquid equilibria data ( $T, x, y$ ) for ternary systems containing ILs. We have not found complete isothermal vapor–liquid equilibria data ( $P, x, y$ ) for ternary systems containing ILs in the literature.

As a continuation of work in a research line recently started consisting of the use of ILs to modify the vapor–liquid equilibria of solvent mixtures that are difficult to separate by distillation, we present in this paper the isobaric vapor–liquid equilibria for chloroform + ethanol + 1-ethyl-3-methylimidazolium trifluoromethanesulfonate ([emim][triflate]) binary and ternary systems at 100 kPa.

The chloroform (1) + ethanol (2) system shows, at atmospheric pressure, a minimum boiling point azeotrope at  $x_1 \approx 0.84$ . Calcium chloride,<sup>22</sup> calcium nitrate,<sup>23</sup> and sodium iodide<sup>23</sup> have been used as entrainers to break the azeotrope, rather unsuccessfully, mainly due to the low solubility of these salts in ethanol and especially in chloroform. As far as we know, no papers reporting the use of ILs to break the azeotrope of the chloroform + ethanol system have been published. Consequently, one of the aims of this work is to determine if [emim][triflate] is also capable of breaking the chloroform + ethanol azeotrope.

## Experimental Section

**Materials.** The solvents used were chloroform (Merck, HPLC grade, minimum mass fraction 99.8 %) and absolute ethanol (Merck, GR grade, minimum mass fraction 99.9 %). No impurities were detected by GC, using the same procedure and conditions described below for liquid mixtures. These chemicals were directly used without further purification. 1-Ethyl-3-methylimidazolium trifluoromethanesulfonate was supplied by Solvent Innovation (Purum, minimum mass fraction 99 %). As said previously,<sup>17</sup> it was selected because of its solubility in both solvents, its low melting point, and its high decomposition

\* To whom correspondence should be addressed. Fax: +34 963 544 898. E-mail: antoni.martinez@uv.es.

temperature which, in case it was used in distillation units, might be easily recovered from column bottoms and reused. Because of its hygroscopic character, it was desiccated at 0.2 Pa overnight prior to use. Prior treatment of the IL before use and its recovering procedure from the VLE apparatus were reported elsewhere.<sup>17</sup>

**Apparatus and Procedure.** Vapor–liquid equilibrium measurements were made with an all-glass dynamic recirculating still (Pilodist, modified Labodest model), equipped with a Cottrell circulation pump.<sup>24</sup> The apparatus has been described in previous papers.<sup>17,25</sup> For vapor–liquid equilibria, every experimental point of the binary chloroform + ethanol system was obtained from an initial sample of pure chloroform at which different quantities of ethanol were added, whereas for the binary chloroform + [emim][triflate] system, starting from an IL concentrated solution, pure chloroform was added until a very diluted solution was achieved. For the ternary system, several ethanol + IL mixtures of known composition were prepared, and different quantities of a mixture of chloroform + IL were added trying to keep the scheduled IL mole fraction in each series. A Mettler AE200 analytical balance with a standard uncertainty of 0.0001 g was used to prepare the samples. Only when constant temperature was reached (30 min or longer) were the equilibrium conditions assumed.

Liquid–liquid binary and ternary equilibrium data were obtained by preparing mixtures with a bulk composition in the immiscibility region which were placed inside of test tubes almost completely filled. The reason for this was to prevent the appearance of an additional vapor phase, which was liable to happen when working at high temperatures. The tested tubes were followed by intense stirring at least for 5 h and maintained at least for 24 h at constant temperature. The temperature was controlled with a thermostatted bath (Unitronic Orbital from Selecta) with an incorporated stirring system. The uncertainty in the temperature measurements was 0.1 K. At the end of the settling period, samples were taken from both phases and analyzed as described below. The time necessary to attain equilibrium, i.e., no variation of composition with time, was established in preliminary experiments.

**Sample Analysis.** The IL mole fraction content in the liquid phase was gravimetrically determined after the volatile components were separated from a known mass of sample (~2.5 g) by evaporation at 393 K until constant mass. Chloroform and ethanol contained in the liquid and condensed vapor phases were analyzed by using a Varian Star 3400 CX gas chromatograph with a thermal conductivity detector (TCD). Details of the chromatographic column, carrier gas, and operating conditions can be seen in a previous paper.<sup>17</sup> A calibration curve was obtained from a set of gravimetrically prepared standard solutions, which allowed us to quantify the amounts of chloroform and ethanol in the samples. As a result of this, the combined standard uncertainty of the mole fraction of the components in the liquid and vapor phases was 0.001.

## Results and Discussion

**Vapor Pressures of Chloroform and Ethanol.** To test the performance of the equilibrium apparatus, vapor pressure of chloroform was measured in the range (305 to 342) K. The Antoine coefficients for chloroform obtained from our experimental data and those obtained for ethanol in a previous work<sup>16</sup> as well as the standard deviations between experimental and calculated vapor pressure data are shown in Table 1. Regarding chloroform, our vapor pressure data and those reported in the literature<sup>26–29</sup> agree on average within 0.20 %. As far as ethanol

**Table 1. Experimental Antoine Coefficients and Mean Absolute Deviations for Chloroform and Ethanol**

component	temperature range/K	Antoine coefficients <sup>a</sup>			$\sigma(P^\circ)^b/\text{kPa}$
		A	B	C	
chloroform	305 to 342	14.0135	2700.34	-46.93	0.033
ethanol	321 to 359	16.8316	3758.56	-43.78	0.018

<sup>a</sup> Antoine equation:  $\ln P^\circ/\text{kPa} = A - B/(T/\text{K} + C)$ . <sup>b</sup>  $\sigma(P^\circ) = [\sum(P^\circ_{\text{expt}} - P^\circ_{\text{calcd}})^2/(N - 3)]^{1/2}$ .

**Table 2. Vapor–Liquid Equilibrium Data for Chloroform (1) + Ethanol (2) at 100 kPa**

$x_1$	$y_1$	$T/\text{K}$	$x_1$	$y_1$	$T/\text{K}$
0.000	0.000	351.20	0.632	0.765	333.03
0.016	0.049	350.29	0.674	0.782	332.78
0.029	0.089	349.54	0.709	0.794	332.59
0.053	0.151	348.30	0.735	0.803	332.49
0.074	0.208	347.13	0.769	0.815	332.34
0.102	0.268	345.70	0.801	0.828	332.24
0.138	0.346	344.13	0.830	0.840	332.24
0.178	0.415	342.39	0.860	0.854	332.20
0.226	0.488	340.48	0.889	0.869	332.27
0.284	0.553	338.66	0.911	0.885	332.37
0.347	0.609	337.04	0.932	0.902	332.53
0.398	0.646	335.84	0.951	0.926	332.77
0.457	0.684	334.92	0.970	0.948	333.07
0.505	0.711	334.29	0.985	0.971	333.44
0.550	0.732	333.75	1.000	1.000	333.96
0.591	0.749	333.35			

is concerned, the agreement with the literature values<sup>30–32</sup> is within 0.40 %.

**Chloroform + Ethanol Binary System.** Vapor–liquid equilibrium for the chloroform (1) + ethanol (2) binary system was measured at 100 kPa, and the experimental results are in Table 2, where  $x_1$  and  $y_1$  are the mole fraction of chloroform in the liquid and vapor phases, respectively, and  $T$  is the equilibrium temperature. This system shows a minimum boiling point azeotrope at  $x_1 = 0.848$  and  $T = 322.20$  K, which can be interpolated from the experimental values. The experimental results for this binary system show a good thermodynamic consistency according to the Van Ness test<sup>33</sup> modified by Fredenslund.<sup>34</sup> The test gave a mean absolute deviation between calculated and measured mole fractions of chloroform in the vapor phase of  $\delta y = 0.0037$ , showing that the values are thermodynamically consistent.

To compare our experimental values with the scarce ones existing in the literature obtained at 101.32 kPa, we have reduced our data to this pressure using the NRTL model as will be described later. At this pressure, our data are in complete agreement within the experimental accuracy with those reported by Morachevskii and Rabinovich<sup>35</sup> and Chen et al.<sup>36</sup> Data reported by Ernst<sup>37</sup> disagree with all experimental sets. Furthermore, despite the existing dispersion, our azeotropic point calculated at 101.32 kPa ( $x_1 = 0.840$ ,  $T = 332.59$  K) agrees with those reported in the literature,<sup>38</sup> which vary within the range  $0.836 > x_1 > 0.849$  and  $332.40 > T/\text{K} > 332.68$ .

**Chloroform + [emim][triflate] Binary System.** Boiling temperatures for chloroform (1) + [emim][triflate] (3) were measured at 100 kPa, and the experimental results are reported in Table 3. In this table,  $x_3$  is the mole fraction of [emim][triflate] in the liquid phase, and  $T$  is the equilibrium temperature.

Following the experimental procedure to obtain the vapor–liquid equilibria data reported before, we observed that for  $x_3 \leq 0.235$  the boiling temperature of solution remained constant within the experimental accuracy and equal to that of pure chloroform. This behavior might be related with the presence of immiscibility between both components. Moreover, when we observed the

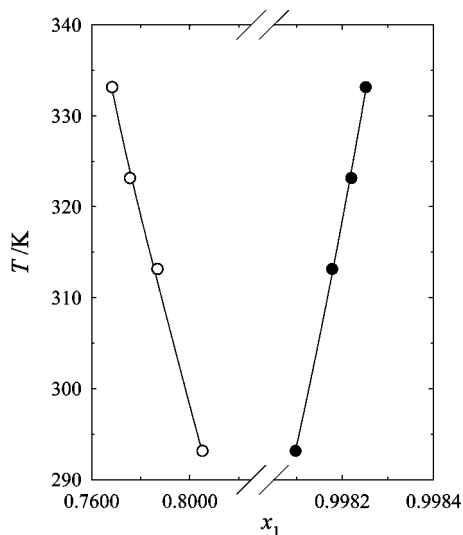
**Table 3.** Vapor–Liquid Equilibrium Data for Chloroform (1) + [emim][triflate] (3) at 100 kPa

$x_3$	$T/K$
0.0000	333.96
0.1554	334.00
0.1978	333.98
0.2185	333.96
0.2342	334.07
0.2523	334.36
0.2706	334.68
0.2810	334.98
0.2952	335.51
0.3106	335.83
0.3284	336.48
0.3491	337.41
0.3585	337.79
0.3724	338.37
0.3881	339.12
0.4014	339.70
0.4204	340.80
0.4289	341.88
0.4524	342.99
0.4666	344.44
0.4709	344.54

**Table 4.** Liquid–Liquid Equilibrium Data for Chloroform (1) + [emim][triflate] (3) at Several Temperatures

$T/K$	[emim][triflate]-rich phase		chloroform-rich phase	
	$x_1$	$x_3$	$x_1$	$x_3$
293.15	0.80519	0.19481	0.99810	0.00190
313.15	0.78685	0.21315	0.99818	0.00182
323.15	0.77563	0.22437	0.99822	0.00178
333.15	0.76840	0.23160	0.99825	0.00175

solution, a light turbidity in the still was found which showed heterogeneity in the liquid phase due to the immiscibility of both components. For this reason, liquid–liquid equilibria of this binary system were measured at (293.15, 313.15, 323.15, and 333.15) K and atmospheric pressure, and the experimental results are reported in Table 4, where  $x_i$  is the mole fraction of component  $i$  in the liquid phase and  $T$  is the equilibrium temperature. These data are drawn in Figure 1, where an immiscibility zone can be seen at high chloroform mole fraction, indicating that [emim][triflate] is practically insoluble in chloroform whereas chloroform is dissolved in [emim][triflate]. In both phases, the immiscibility increases with temperature. For

**Figure 1.** Equilibrium composition of liquid phases for the chloroform (1) + [emim][triflate] (3) system at several temperatures: ●, chloroform-rich phase; ○, [emim][triflate]-rich phase.**Table 5.** Mole Fraction Compositions of the Experimental Tie-Line Ends for the Ternary System Chloroform (1) + Ethanol (2) + [emim][triflate] (3) at (293.15 and 323.15) K

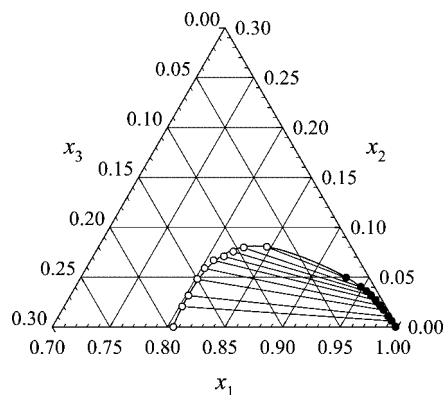
$T/K$	[emim][triflate]-rich phase			chloroform-rich phase		
	$x_1$	$x_2$	$x_3$	$x_1$	$x_2$	$x_3$
293.15	0.8052	0.0000	0.1948	0.9981	0.0000	0.0019
	0.8026	0.0204	0.1770	0.9915	0.0061	0.0024
	0.8024	0.0315	0.1661	0.9864	0.0107	0.0029
	0.8020	0.0479	0.1501	0.9793	0.0169	0.0038
	0.8028	0.0588	0.1385	0.9737	0.0216	0.0047
	0.8067	0.0668	0.1265	0.9672	0.0269	0.0059
	0.8137	0.0707	0.1156	0.9609	0.0317	0.0074
	0.8195	0.0755	0.1051	0.9548	0.0358	0.0093
	0.8264	0.0795	0.0941	0.9478	0.0401	0.0122
	0.8461	0.0803	0.0736	0.9305	0.0493	0.0201
323.15	0.7756	0.0000	0.2244	0.9982	0.0000	0.0018
	0.7745	0.0160	0.2095	0.9920	0.0058	0.0022
	0.7736	0.0294	0.1971	0.9861	0.0114	0.0025
	0.7750	0.0446	0.1804	0.9776	0.0192	0.0032
	0.7740	0.0529	0.1731	0.9731	0.0232	0.0037
	0.7777	0.0626	0.1597	0.9665	0.0291	0.0044
	0.7801	0.0716	0.1484	0.9594	0.0351	0.0055
	0.7826	0.0759	0.1414	0.9554	0.0383	0.0062
	0.7847	0.0806	0.1347	0.9513	0.0417	0.0070
	0.7917	0.0867	0.1216	0.9424	0.0487	0.0089
0.7967	0.0922	0.1111	0.9340	0.0559	0.0100	
0.8051	0.0950	0.0999	0.9266	0.0607	0.0127	
0.8177	0.0966	0.0856	0.9115	0.0691	0.0193	

values of  $x_1 < 0.765$  ( $x_3 > 0.235$ ), the miscibility of both components is total. None of these problems were detected with ethanol + [emim][triflate] binary mixtures.<sup>16</sup>

#### Chloroform + Ethanol + [emim][triflate] System.

Liquid–liquid equilibria for the chloroform (1) + ethanol (2) + [emim][triflate] (3) system were measured at (293.15 and 323.15) K, following the experimental procedure described before. The experimental results are reported in Table 5, and they are shown in Figures 2 and 3, where only the chloroform-rich corner has been drawn for clarity. In these figures, it can be observed that the small immiscible region, which increases with temperature, is placed at the highest chloroform compositions. The ternary system is totally miscible for  $x_2 > 0.100$  or  $x_3 > 0.235$  at a temperature range of (293.15 to 323.15) K.

Vapor–liquid equilibria for the chloroform (1) + ethanol (2) + [emim][triflate] (3) system, at 100 kPa, were obtained by trying to keep the IL mole fraction constant in each of the four series at  $x_3 \approx 0.05, 0.13, 0.21,$  and  $0.32$ . In Figure 4, we have drawn on a ternary diagram the location of the liquid-phase composition for the experimental points taken in each series, as well as the immiscibility area at (293.15 and 323.15) K. In

**Figure 2.** Liquid–liquid equilibrium data for the chloroform (1) + ethanol (2) + [emim][triflate] (3) system at 293.15 K: ●, chloroform-rich phase; ○, [emim][triflate]-rich phase; —, experimental tie lines.

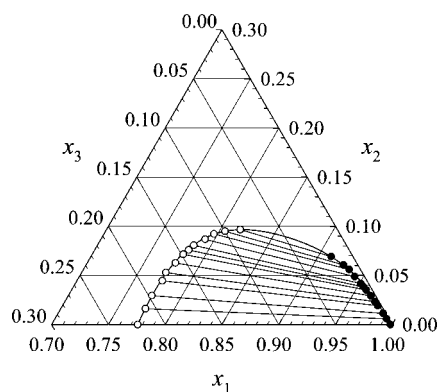


**Figure 3.** Liquid–liquid equilibrium data for the chloroform (1) + ethanol (2) + [emim][triflate] (3) system at 323.15 K: ●, chloroform-rich phase; ○, [emim][triflate]-rich phase; –, experimental tie lines.

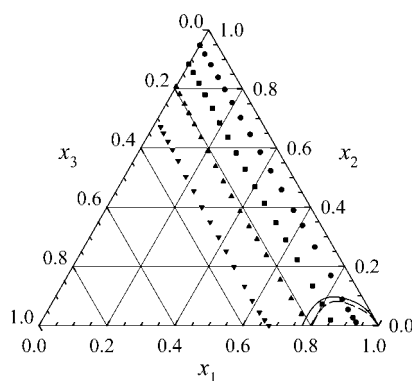


**Figure 4.** Location of the liquid-phase composition for the experimental points taken to determine the vapor–liquid equilibrium for the chloroform (1) + ethanol (2) + [emim][triflate] (3) system: ●,  $x_3 = 0.05$ ; ■,  $x_3 = 0.13$ ; ▲,  $x_3 = 0.21$ ; ▼,  $x_3 = 0.32$ ; solid line represents immiscible zone at 323.15 K; dashed line represents immiscible zone at 293.15 K.

this figure, it can be observed that the series having the least IL composition ( $x_3 = 0.05$ ) exhibits immiscibility in the liquid phase for the last four points. The  $x_3 = 0.13$  series presents immiscibility for two points only, whereas the series with higher IL composition exhibits total liquid-phase miscibility. Despite the immiscibility found in some points, we had no problems with the liquid-phase analysis because they presented emulsification (very small droplets dispersed in a liquid phase), and therefore samples taken with a syringe ( $\sim 2.5$  g) had a reproducible composition.

In this way, the experimental values of the vapor–liquid equilibrium for the ternary system are shown in Table 6, where  $x_3$  is the mole fraction of [emim][triflate] in the liquid phase;  $x_1'$  is the mole fraction of chloroform in the liquid phase expressed on an IL-free basis;  $y_1$  is the mole fraction of chloroform in the vapor phase; and  $T$  is the equilibrium temperature.

**Modeling the Vapor–Liquid Phase Equilibrium.** As indicated in previous papers,<sup>14–17</sup> we have used the electrolyte NRTL model to fit the vapor–liquid equilibrium of the IL-containing ternary system. This model is an extension of the nonrandom two-liquid local composition proposed by Renon and Prausnitz<sup>39</sup> for liquid-phase activity coefficients. Chen et al.<sup>40</sup> derived a model for single-solvent + electrolyte systems, and later Mock et al.<sup>41,42</sup> extended it to mixed-solvent + electrolyte systems, by neglecting the long-range interaction contribution term.

It is expressions for the liquid-phase activity coefficients of chloroform (1) and ethanol (2) in a binary or ternary system

**Table 6.** Vapor–Liquid Equilibrium Data for Chloroform (1) + Ethanol (2) + [emim][triflate] (3) at 100 kPa

$x_3$	$x_1'$	$y_1$	$T/K$
0.0525	0.000	0.000	352.28
0.0532	0.031	0.091	350.53
0.0535	0.069	0.188	348.52
0.0537	0.114	0.284	346.33
0.0541	0.157	0.372	344.53
0.0545	0.204	0.449	342.46
0.0550	0.257	0.516	340.47
0.0555	0.316	0.578	338.64
0.0557	0.380	0.633	336.97
0.0558	0.446	0.685	335.58
0.0561	0.514	0.725	334.47
0.0559	0.587	0.758	333.59
0.0554	0.642	0.784	333.00
0.0548	0.719	0.818	332.53
0.0561	0.821	0.864	332.28
0.0628	0.906	0.907	332.41
0.0626	0.943	0.929	332.72
0.0627	0.972	0.953	333.14
0.0611	0.989	0.974	333.39
0.0600	1.000	1.000	333.96
0.1170	0.000	0.000	353.50
0.1183	0.030	0.078	351.78
0.1195	0.069	0.175	349.92
0.1210	0.113	0.271	347.89
0.1217	0.164	0.365	345.68
0.1247	0.217	0.447	343.62
0.1259	0.272	0.522	341.67
0.1272	0.331	0.585	339.88
0.1287	0.393	0.641	338.15
0.1292	0.461	0.696	336.59
0.1290	0.525	0.738	335.31
0.1285	0.601	0.781	334.16
0.1286	0.669	0.813	333.40
0.1273	0.744	0.848	332.83
0.1276	0.847	0.893	332.57
0.1296	0.916	0.926	332.84
0.1314	0.978	0.969	333.38
0.1300	1.000	1.000	333.96
0.1920	0.000	0.000	355.12
0.1948	0.029	0.066	353.44
0.1970	0.067	0.150	351.91
0.1998	0.103	0.229	350.36
0.2026	0.148	0.321	348.53
0.2050	0.200	0.409	346.61
0.2082	0.256	0.483	344.84
0.2111	0.318	0.551	342.92
0.2136	0.380	0.616	341.30
0.2149	0.444	0.674	339.69
0.2150	0.509	0.722	338.26
0.2136	0.574	0.766	336.95
0.2118	0.629	0.802	335.94
0.2116	0.699	0.837	334.97
0.2122	0.804	0.889	334.03
0.2117	0.885	0.932	333.52
0.2081	0.951	0.968	333.43
0.2185	1.000	1.000	333.96
0.3062	0.000	0.000	358.60
0.3064	0.033	0.076	356.81
0.3078	0.060	0.139	355.77
0.3088	0.099	0.214	354.33
0.3093	0.140	0.286	352.74
0.3114	0.192	0.373	350.95
0.3155	0.264	0.474	349.09
0.3171	0.335	0.557	347.16
0.3204	0.412	0.628	345.22
0.3209	0.485	0.691	343.38
0.3217	0.560	0.749	341.81
0.3234	0.629	0.795	340.65
0.3268	0.707	0.840	339.48
0.3286	0.804	0.891	338.29
0.3305	0.876	0.928	337.39
0.3288	0.935	0.961	336.78
0.3260	0.973	0.984	336.56
0.3228	1.000	1.000	336.26



**Table 7. Estimated Values of Nonrandomness Factors,  $\alpha_{i,j}$ , and Energy Parameters,  $\Delta g_{i,j}$  and  $\Delta g_{j,i}$ , for the Electrolyte NRTL Model**

<i>i</i> component	<i>j</i> component	$\alpha_{i,j}$	$\Delta g_{i,j}/J \cdot \text{mol}^{-1}$	$\Delta g_{j,i}/J \cdot \text{mol}^{-1}$
chloroform	ethanol	0.146	8398.9	-3494.4
chloroform	[emim][triflate]	0.591	11088.6	692.2
ethanol	[emim][triflate]	0.772	7072.8	-566.6

containing [emim][triflate] (3) that the model produces. These equations have been reported in a previous paper.<sup>43</sup> Accordingly, we have to determine the nine binary adjustable parameters for all the solvent + solvent and solvent + electrolyte pairs in the system to represent the phase equilibrium of mixed-solvent + electrolyte systems.

The (1–2) binary solvent–solvent parameters were obtained applying the model to the vapor–liquid equilibria data of the chloroform (1) + ethanol (2) system shown in Table 2 by minimization of the objective function  $F_1$

$$F_1 = \sum_N (T_{\text{exptl}} - T_{\text{calcd}})^2 \quad (1)$$

where  $T$  is the equilibrium temperature; the indices exptl and calcd denote the experimental and calculated values, respectively; and the summations are extended to the whole range of data points. These parameters are reported in Table 7.

Regarding the parameters corresponding to the 1–3 binary solvent–IL pair, we have to stress that they could not be estimated from the vapor–liquid equilibria data of the chloroform (1) + [emim][triflate] (3) binary system because the observed immiscibility in this system resulted in a constant boiling point at  $x_3 < 0.235$  as pointed above, which made it impossible for the model to determine these parameters.

Because of that, the parameters corresponding to the binary solvent–IL pairs had to be established from the experimental vapor–liquid equilibrium data of the chloroform (1) + ethanol (2) + [emim][triflate] (3) system and the electrolyte NRTL model. Thus, the model was applied by taking into account the (1–2) binary parameters from the previous adjustment, whereas those corresponding to the (1–3) and (2–3) binary system were obtained by minimization of the objective function  $F_2$

$$F_2 = \sum_N \left[ \left( 1 - \frac{\gamma_{1,\text{calcd}}}{\gamma_{1,\text{exptl}}} \right)^2 + \left( 1 - \frac{\gamma_{2,\text{calcd}}}{\gamma_{2,\text{exptl}}} \right)^2 \right] \quad (2)$$

where  $\gamma_i$  is the activity coefficient of solvent  $i$ ; the indices exptl and calcd denote the experimental and calculated values, respectively; and the summations are extended to the whole range of data points.

Following this procedure, we were able to determine the parameters of the model, and their values are reported in Table 7. These parameters were obtained by assuming ideal behavior for the vapor phase and iteratively solving the equilibrium conditions expressed in eq 3 for the solvent.

$$y_i P = X_i \gamma_i P_i^o \quad (3)$$

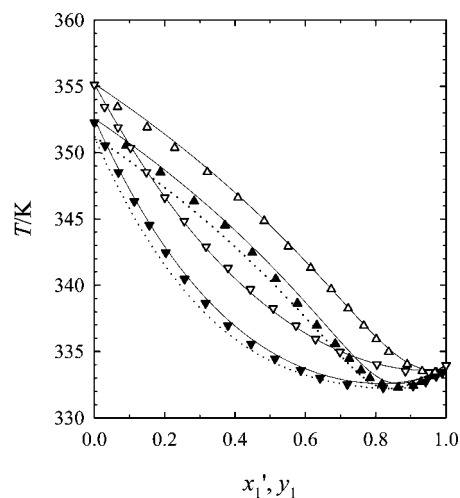
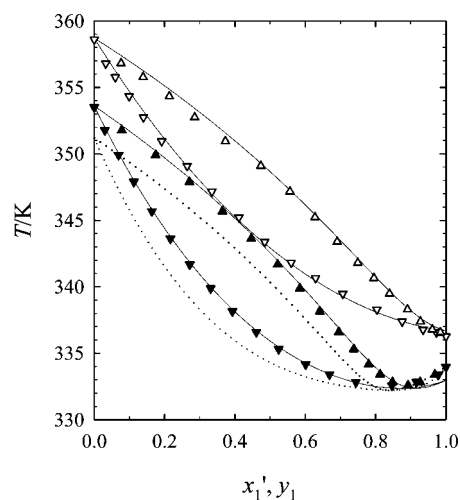
where  $y_i$  is the vapor phase mole fraction of solvent  $i$ ;  $P$  is the total pressure in the system;  $X_i$  is the liquid phase mole fraction of solvent  $i$  calculated as if total dissociation of electrolytes had happened;  $\gamma_i$  is the activity coefficient of component  $i$  obtained from the electrolyte NRTL model; and  $P_i^o$  is the vapor pressure of solvent  $i$  at equilibrium temperature. The vapor pressures of pure solvents were calculated using the Antoine coefficients given in Table 1.

With the electrolyte NRTL model and the parameters shown in Table 7, it is possible to calculate the composition in the

**Table 8. Mean Absolute Deviations,  $\delta y$  and  $\delta T$ , and Standard Deviations,  $\sigma y$  and  $\sigma T$ , between Experimental and Calculated Values of the Vapor–Phase Mole Fractions and the Equilibrium Temperatures**

system	$\delta y^a$	$\sigma y^b$	$\delta T^c/K$	$\sigma T^d/K$
chloroform + ethanol	0.005	0.006	0.13	0.17
chloroform + ethanol + [emim][triflate]	0.009	0.010	0.21	0.29

<sup>a</sup>  $\delta y = (1/N) \sum |y_{\text{exptl}} - y_{\text{calcd}}|$ . <sup>b</sup>  $\sigma y = [\sum (y_{\text{exptl}} - y_{\text{calcd}})^2 / (N - m)]^{1/2}$ . <sup>c</sup>  $\delta T = (1/N) \sum |T_{\text{exptl}} - T_{\text{calcd}}|$ . <sup>d</sup>  $\sigma T = [\sum (T_{\text{exptl}} - T_{\text{calcd}})^2 / (N - m)]^{1/2}$ .  $N$  is the number of experimental points, and  $m$  is the number of parameters for the model.

**Figure 5.** Temperature–composition diagram for chloroform (1) + ethanol (2) + [emim][triflate] (3) at 100 kPa, at several mole fractions of IL:  $\blacktriangledown$ ,  $x_1'$  experimental at  $x_3 = 0.05$ ;  $\blacktriangle$ ,  $y_1$  experimental at  $x_3 = 0.05$ ;  $\nabla$ ,  $x_1'$  experimental at  $x_3 = 0.21$ ;  $\triangle$ ,  $y_1$  experimental at  $x_3 = 0.21$ ; solid lines, calculated; dotted lines, calculated for IL-free system.**Figure 6.** Temperature–composition diagram for chloroform (1) + ethanol (2) + [emim][triflate] (3) at 100 kPa, at several mole fractions of IL:  $\blacktriangledown$ ,  $x_1'$  experimental at  $x_3 = 0.13$ ;  $\blacktriangle$ ,  $y_1$  experimental at  $x_3 = 0.13$ ;  $\nabla$ ,  $x_1'$  experimental at  $x_3 = 0.32$ ;  $\triangle$ ,  $y_1$  experimental at  $x_3 = 0.32$ ; solid lines, calculated; dotted lines, calculated for IL-free system.

vapor phase and equilibrium temperature for each composition in the liquid phase. In this way, the standard and mean absolute deviations between the experimental and calculated values of molar fraction in the vapor phase and equilibrium temperature for binary and ternary systems were calculated and are reported in Table 8.

In Figures 5 and 6, the calculated and experimental vapor–liquid equilibrium of the chloroform (1) + ethanol (2) + [emim][triflate] (3) points are plotted on  $(T, x_1', y_1)$  diagrams

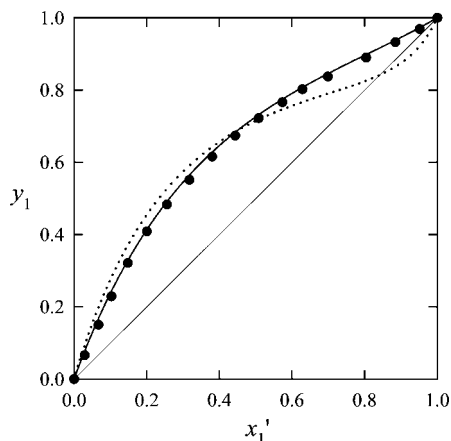


**Figure 7.** Salting-out effect of [emim][triflate] on vapor–liquid equilibrium of the chloroform (1) + ethanol (2) system at 100 kPa for an IL mole fraction  $x_3 = 0.21$ : ●, experimental value; solid line, calculated with the electrolyte NRTL model; dotted line, calculated for IL-free system.

for  $x_3 = 0.05, 0.13, 0.21,$  and  $0.32$ . The model is seen to be able to properly fit the experimental vapor–liquid equilibrium data, except for the immiscibility zone ( $x_3 < 0.235, x_1' > 0.900$ ), because inside it the model predicts unrealistic boiling point temperatures keeping the temperature actually constant, as seen for the  $x_3 = 0.13$  series at high chloroform composition. Perhaps the fact that in ternary systems an only set of model parameters suitably describing the vapor–liquid–liquid equilibrium<sup>44</sup> does not exist may explain this situation. The  $x_3 = 0.05$  series should also present the same behavior, but fortuitously and only exactly for this IL composition, the model reproduces the boiling point of the mixtures.

Ethanol is more polar than chloroform. Hence, chloroform is supposed to be salted-out from the mixed solvent over the whole range of liquid concentration. However, we only note an appreciable salting-out effect when chloroform mole fractions in the liquid phase are higher than 0.5, whereas a minor salting-in effect appears at lower compositions. This can be observed in Figure 7, where only experimental and calculated data for  $x_3 = 0.21$  have been plotted for clarity. [emim][triflate] produces a crossover effect,<sup>45</sup> between salting-in and salting-out in the chloroform + ethanol system, higher than that observed in the acetone + methanol,<sup>14</sup> methyl acetate + methanol,<sup>15</sup> or ethyl acetate + ethanol<sup>16</sup> systems with the same IL, although smaller than that observed in the 1-propanol + water<sup>17</sup> system.

It is worth noting too that an increase in the [emim][triflate] concentration produces a displacement of the azeotropic point of the chloroform + ethanol system toward  $x_1' > 0.848$ . Experimentally, by using an [emim][triflate] mole fraction  $x_3 = 0.13$ , the azeotrope has not yet disappeared, whereas it has already disappeared for  $x_3 = 0.21$ .

The model failure at the described immiscibility conditions does not affect its predictive capacity because the ternary system is totally miscible for the IL composition required to break the azeotrope, and therefore the calculated values using the electrolyte NRTL model agree with the experimental ones.

## Conclusions

In this work, vapor–liquid equilibria at 100 kPa and liquid–liquid equilibria at various temperatures for chloroform + [emim][triflate] and chloroform + ethanol + [emim][triflate] systems have been determined.

The chloroform (1) + ethanol (2) + [emim][triflate] (3) ternary system presents an immiscibility region, which increases

with the temperature, placed at the highest chloroform compositions. The ternary system is totally miscible for  $x_2 > 0.100$  or  $x_3 > 0.235$  at the temperature range (293.15 to 323.15) K.

The electrolyte NRTL model is suitable to predict the VLE in the presence of an IL such as [emim][triflate] whenever the ternary system is totally miscible. Although an immiscibility zone is present, the model is suitable outside of this zone. In this way, this will allow us to extend the application of the model to the field of ionic liquids.

The addition of [emim][triflate] to the chloroform + ethanol mixture gives a considerable salting-out effect on chloroform near the azeotropic point, although a slight salting-in effect at low chloroform concentrations occurs. At 100 kPa, the azeotrope is removed at an [emim][triflate] mole fraction of  $x_3 = 0.21$ . This IL is also capable of breaking the azeotrope of the acetone + methanol,<sup>14</sup> methyl acetate + methanol,<sup>15</sup> and ethyl acetate + ethanol<sup>16</sup> systems.

## Literature Cited

- (1) Seddon, K. R. Ionic liquids for clean technology. *J. Chem. Technol. Biotechnol.* **1997**, *68*, 351–356.
- (2) Lei, Z.; Chen, B.; Ding Z. *Special Distillation Processes*; Elsevier: Amsterdam, 2005.
- (3) Marsh, K. N.; Boxall, J. A.; Lichtenthaler, R. Room temperature ionic liquids and their mixtures—a review. *Fluid Phase Equilib.* **2004**, *219*, 93–98.
- (4) Seiler, M.; Jork, C.; Kavarnou, A.; Arlt, W.; Hirsch, R. Separation of azeotropic mixtures using hyperbranched polymers or ionic liquids. *AIChE J.* **2004**, *50*, 2439–2454.
- (5) Jork, C.; Seiler, M.; Beste, Y. A.; Arlt, W. Influence of ionic liquids on the phase behavior of aqueous azeotropic systems. *J. Chem. Eng. Data* **2004**, *49*, 852–857.
- (6) Beste, Y.; Eggersmann, M.; Schoenmakers, H. Extractive distillation with ionic fluids. *Chem. Ing. Tech.* **2005**, *77*, 1800–1808.
- (7) Lei, Z.; Arlt, W.; Wasserscheid, P. Separation of 1-hexene and n-hexane with ionic liquids. *Fluid Phase Equilib.* **2006**, *241*, 290–299.
- (8) Lei, Z.; Arlt, W.; Wasserscheid, P. Selection of entrainers in the 1-hexene/n-hexane system with a limited solubility. *Fluid Phase Equilib.* **2007**, *260*, 29–35.
- (9) Zhao, J.; Dong, C. C.; Li, C. X.; Meng, H.; Wang, Z. H. Isobaric vapor–liquid equilibria for ethanol–water system containing different ionic liquids at atmospheric pressure. *Fluid Phase Equilib.* **2006**, *242*, 147–153.
- (10) Zhao, J.; Li, C.; Wang, Z. Vapor pressure measurement and prediction for ethanol + methanol and ethanol + water systems containing ionic liquids. *J. Chem. Eng. Data* **2006**, *51*, 1755–1760.
- (11) Calvar, N.; González, B.; Gómez, E.; Domínguez, A. Vapor–liquid equilibria for the ternary system ethanol + water + 1-butyl-3-methylimidazolium chloride and the corresponding binary systems at 101.3 kPa. *J. Chem. Eng. Data* **2006**, *51*, 2178–2181.
- (12) Calvar, N.; González, B.; Gómez, E.; Domínguez, A. Study of the behaviour of the azeotropic mixture ethanol–water with imidazolium-based ionic liquids. *Fluid Phase Equilib.* **2007**, *259*, 51–56.
- (13) Calvar, N.; González, B.; Gómez, E.; Domínguez, A. Vapor–liquid equilibria for the ternary system ethanol + water + 1-ethyl-3-methylimidazolium ethylsulfate and the corresponding binary systems containing the ionic liquid at 101.3 kPa. *J. Chem. Eng. Data* **2008**, *53*, 820–825.
- (14) Orchillés, A. V.; Miguel, P. J.; Vercher, E.; Martínez-Andreu, A. Ionic liquids as entrainers in extractive distillation: isobaric vapor–liquid equilibria for acetone + methanol + 1-ethyl-3-methylimidazolium trifluoromethanesulfonate. *J. Chem. Eng. Data* **2007**, *52*, 141–147.
- (15) Orchillés, A. V.; Miguel, P. J.; Vercher, E.; Martínez-Andreu, A. Isobaric vapor–liquid equilibria for ethyl acetate + ethanol + 1-ethyl-3-methylimidazolium trifluoromethanesulfonate at 100 kPa. *J. Chem. Eng. Data* **2007**, *52*, 915–920.
- (16) Orchillés, A. V.; Miguel, P. J.; Vercher, E.; Martínez-Andreu, A. Isobaric vapor–liquid equilibria for 1-propanol + water + 1-ethyl-3-methylimidazolium trifluoromethanesulfonate at 100 kPa. *J. Chem. Eng. Data* **2007**, *52*, 2325–2330.
- (17) Orchillés, A. V.; Miguel, P. J.; Vercher, E.; Martínez-Andreu, A. Isobaric vapor–liquid equilibria for 1-propanol + water + 1-ethyl-3-methylimidazolium trifluoromethanesulfonate at 100 kPa. *J. Chem. Eng. Data* **2008**, doi:10.1021/jc800436u.

- (18) Zhang, L. Z.; Deng, D. S.; Han, J. Z.; Ji, D. X.; Ji, J. B. Isobaric vapor–liquid equilibria for water + 2-propanol + 1-butyl-3-methylimidazolium tetrafluoroborate. *J. Chem. Eng. Data* **2007**, *52*, 199–205.
- (19) Zhang, L. Z.; Han, J. Z.; Wang, R. J.; Qiu, X. Y.; Ji, J. B. Isobaric vapor–liquid equilibria for three ternary systems: water + 2-propanol + 1-ethyl-3-methylimidazolium tetrafluoroborate, water + 1-propanol + 1-ethyl-3-methylimidazolium tetrafluoroborate, and water + 1-propanol + 1-butyl-3-methylimidazolium tetrafluoroborate. *J. Chem. Eng. Data* **2007**, *52*, 1401–1407.
- (20) Zhang, L.; Yuan, X.; Qiao, B.; Qi, R.; Ji, J. Isobaric vapor–liquid equilibria for water + ethanol + ethyl acetate + 1-butyl-3-methylimidazolium acetate at low water mole fractions. *J. Chem. Eng. Data* **2008**, *53*, 1595–1601.
- (21) Li, Q.; Xing, F.; Lei, Z.; Wang, B.; Chang, Q. Isobaric vapor–liquid equilibrium for isopropanol + water + 1-ethyl-3-methylimidazolium tetrafluoroborate. *J. Chem. Eng. Data* **2008**, *53*, 275–279.
- (22) Darwish, N. A.; Al-Anber, Z. A. Isobaric vapor–liquid equilibria of chloroform + ethanol and chloroform + ethanol + calcium chloride at 94.0 kPa. *Fluid Phase Equilib.* **1997**, *131*, 259–267.
- (23) Whittwer, F.; Rose, C. *Dortmund Data Bank V5.0*; DDB: Oldenburg, Germany, 2007.
- (24) Walas, S. M. *Phase Equilibria in Chemical Engineering*; Butterworth: London, 1985.
- (25) Vercher, E.; Orchillés, A. V.; Miguel, P. J.; González-Alfaro, V.; Martínez-Andreu, A. Isobaric vapor–liquid equilibria for acetone + methanol + lithium nitrate at 100 kPa. *Fluid Phase Equilib.* **2006**, *250*, 131–137.
- (26) Scatchard, G.; Raymond, C. L. Vapor–liquid equilibrium. II. Chloroform-ethanol mixtures at 35, 45 and 55°. *J. Am. Chem. Soc.* **1938**, *60*, 1278–1287.
- (27) Kudryavtseva, L. S.; Susarev, M. P. Liquid-vapor equilibrium in systems chloroform-hexane and acetone-chloroform. *Zh. Prikl. Khim. (Leningrad)* **1963**, *36*, 1231–1237.
- (28) Boublik, T.; Aim, K. Heats of vaporization of simple non-spherical molecule compounds. *Collect. Czech. Chem. Commun.* **1972**, *37*, 3513–3521.
- (29) Segura, H.; Mejia, A.; Reich, R.; Wisniak, J.; Loras, S. Isobaric vapor–liquid equilibria and densities for the binary systems oxolane + ethyl 1,1-dimethylethyl ether, oxolane + 2-propanol and propan-2-one + trichloromethane. *Phys. Chem. Liq.* **2003**, *41*, 283–301.
- (30) Figurski, G.; Malanowski, S. K. Vapor–liquid equilibrium studies of the ethanol + ethyl acetate system. *Fluid Phase Equilib.* **1988**, *148*, 161–169.
- (31) Mund, W.; Heim, G. Vapor tensions of the system: ethyl alcohol-ethyl acetate. *Bull. Soc. Chim. Belg.* **1932**, *41*, 349–376.
- (32) Ambrose, D.; Sprake, C. H. S. Thermodynamic properties of organic oxygen compounds XXV. Vapour pressures and normal boiling temperatures of aliphatic alcohols. *J. Chem. Thermodyn.* **1970**, *2*, 631–645.
- (33) Van Ness, H. C.; Byer, S. M.; Gibbs, R. E. Vapor–liquid equilibrium: part I. An appraisal of data reduction methods. *AIChE J.* **1973**, *19*, 238–244.
- (34) Fredenslund, A.; Gmehling, J.; Rasmussen, P. *Vapor–Liquid Equilibria Using UNIFAC*; Elsevier: Amsterdam, 1977.
- (35) Morachevskii, A. G.; Rabinovich, R. Sh. Liquid-vapor equilibrium in the chloroform-ethyl alcohol system. *Zh. Prikl. Khim. (Leningrad)* **1959**, *32*, 458–459.
- (36) Chen, G.-H.; Wang, Q.; Ma, Z.-M.; Yan, X.-H.; Han, S.-J. Phase equilibria at superatmospheric pressures for systems containing halohydrocarbon, aromatic hydrocarbon, and alcohol. *J. Chem. Eng. Data* **1995**, *40*, 361–366.
- (37) Ernst, P. Master's Thesis, Universitat Dortmund: Dortmund, Germany, 1975.
- (38) Gmehling, J.; Menke, J.; Krafczyk, J.; Fischer, K. *Azeotropic Data*; VCH: Weinheim, 1994.
- (39) Renon, H.; Prausnitz, J. M. Local compositions in thermodynamic excess functions for liquid mixtures. *AIChE J.* **1968**, *14*, 135–144.
- (40) Chen, C. C.; Britt, H. I.; Boston, J. F.; Evans, L. B. Local composition model for excess Gibbs energy of electrolyte systems. Part I: single solvent, single completely dissociated electrolyte systems. *AIChE J.* **1982**, *28*, 588–596.
- (41) Mock, B.; Evans, L. B.; Chen, C. C. Phase equilibria in multiple-solvent electrolyte systems: a new thermodynamic model. *Proc. Summer Comput. Simul. Conf.* 1984, 558–562.
- (42) Mock, B.; Evans, L. B.; Chen, C. C. Thermodynamic representation of phase equilibria of mixed-solvent electrolyte systems. *AIChE J.* **1986**, *32*, 1655–1664.
- (43) Vercher, E.; Rojo, F. J.; Martínez-Andreu, A. Isobaric vapor–liquid equilibria for 1-propanol + water + calcium nitrate. *J. Chem. Eng. Data* **1999**, *44*, 1216–1221.
- (44) Chen, C. C.; Mathias, P. M. Applied thermodynamics for process modeling. *AIChE J.* **2002**, *48*, 194–200.
- (45) Miranda, D.; Furter, W. F. Salt effects on VLE: some anomalies. *AIChE J.* **1974**, *20*, 103–108.

Received for review July 14, 2008. Accepted September 3, 2008. This research was supported by the Ministry of Education and Science of Spain and FEDER funds of the European Union, through Project no. CTQ2007-60831/PPQ.

JE800548T